INTERNATIONAL JOURNAL OF ROBUST AND NONLINEAR CONTROL
Int. J. Robust. Nonlinear Control 20xx; **00**:1–26
Published online in Wiley InterScience (www.interscience.wiley.com). DOI: 10.1002/rnc

Iterative feedback tuning for Hamiltonian systems based on variational symmetry

Satoshi Satoh[1]*and Kenji Fujimoto[2]

[1]*Department of Mechanical Engineering, Graduate School of Engineering, Osaka University, 2-1, Yamadaoka, Suita, Osaka 565-0871, Japan* [2]*Department of Aerospace Engineering, Graduate School of Engineering, Kyoto University, Yoshida-Honmachi, Sakyo-ku, Kyoto 606-8501, Japan*

SUMMARY

This paper proposes a novel iterative feedback tuning (IFT) for Hamiltonian systems, which can describe a practically important class of nonlinear systems. Hamiltonian systems have a special property called variational symmetry, and it can be used to estimate the input-output mapping of the variational adjoint for certain input-output mappings of the systems. First, we derive a modified variational symmetry to adapt to the gradient estimation of an optimal control type cost function with respect to adjustable parameters of a controller. Second, we provide an IFT algorithm based on the property, which generates the optimal parameters minimizing the cost function by iteration of experiments. The proposed algorithm requires less number of experiments to estimate the gradient than the conventional IFT methods for nonlinear systems. We also provide a method to optimize the elements of the dissipation matrix, which does not directly appear in the Hamiltonian function, by equipping a dynamic feedback of the generalized coordinate. Moreover, we provide an IFT algorithm considering parameter constraints so that the parameters can be optimized within a prescribed search range. Finally, a numerical simulation of a two-link robot manipulator including comparison with the conventional IFT methods, demonstrate the effectiveness of the proposed method.

Received . . .

KEY WORDS: Iterative feedback tuning, Nonlinear control, Hamiltonian systems, Variational symmetry

1. INTRODUCTION

In the research area on control of physical systems, most of the existing results focus on feedback stabilization and related topics such as trajectory tracking control, output feedback control and so on. They utilize physical properties such as passivity and symmetry for control effectively [1, 2, 3, 4, 5, 6]. In those methods, a precise model of the plant system is required. However, it is quite difficult to construct a precise model for a given plant system, and it is always required to adjust the design parameters when we design a control system. Hence, it is desired to adjust/generate a feedback controller or feedforward input by automatic learning. For this purpose, several methods

*Correspondence to: Osaka University, 2-1, Yamadaoka, Suita, Osaka 565-0871, Japan. E-mail: s.satoh@ieee.org

have been proposed. In control engineering, iterative learning control (ILC) [7, 8, 9, 10] and iterative feedback tuning (IFT) [11, 12, 13, 14, 15] are well known. ILC is to generate a feedforward input to achieve a given desired trajectory by iteration of experiments and IFT adjusts the design parameters of a feedback controller via experiments.

Since this paper is particularly concerned with IFT and proposes a novel IFT algorithm utilizing a special property of physical systems, we further focus on the conventional IFT methods. There are many results reported on IFT, e.g., [11, 16, 12, 17, 13, 14, 15]. A common control strategy for an IFT problem is to select a cost function as optimal control, and to adjust parameters of the feedback controller so that the cost function decreases. In this approach, the gradient of the cost function with respect to the parameter is estimated using input-output (I/O) data. One possible issue of IFT is that it basically requires a number of experiments in order to execute one step optimization in the gradient method compared with ILC, where one step optimization requires only one experiment. Regarding this, for the IFT methods of linear systems [11, 12, 13, 14], an efficient tuning algorithm is proposed, which reduces the number of experiments required for the gradient calculation by using commutativity of linear operators. On the contrary, some researchers extend the IFT method to nonlinear systems, e.g., [16, 17, 15]. However, the aforementioned commutativity does not hold any more, and thus the required number of the gradient experiments per one step optimization is equal to the number of tuning parameters in [16, 17, 15]. Besides, although the literature [17] also provides an alternative IFT method, which requires only two gradient experiments per one step optimization, it requires identification of a model of the linearized closed-loop system around its operating trajectory, instead. Another approach is proposed in the literature [18] based on the multi-parametric extremum seeking (MES) method. MES allows to require only one gradient experiment per one step optimization. Since, however, this method requires carefully chosen dither signals, instead, it is only guaranteed that the average of each parameter signal contaminated with dither signals converges to the optimal one. The literature [19] proposes a passivity-based stabilizing controller design for physical systems using the actor-critic method. In general, the passivity-based controller requires to solve a pair of partial differential equations with respect to coordinate transformation, additional energy function and dissipation matrix [2, 3]. Here, additional energy function and dissipation matrix are linearly parameterized with known basis functions, and they are learned without solving the partial differential equations. However, the original physical system model is required, and the optimality of the controller itself is not considered. On the contrary, the proposed method is applicable to a practically important class of nonlinear systems, guarantees the optimality of the resultant controller, and can reduce the necessary gradient experiments without using the plant model nor dither signals by making use of a special property of physical systems.

So far, we have developed an ILC method for Hamiltonian systems [20, 21, 22]. The conventional ILC methods rely on the problem setting of trajectory tracking control, and they are not applicable to other problems such as trajectory generation. The authors' former results are based on a special property of the Hamiltonian systems called variational symmetry, and they are applicable to a wide class of problems described by cost functions of optimal control type. The most original feature of the proposed IFT in this paper is to enjoy significant benefits of using the variational symmetry in the IFT algorithm. First, we investigate a modified variational symmetry of Hamiltonian systems, which can be adapted to optimization of finite number of parameters. Second, a novel IFT method is constructed based on this property. The proposed IFT method requires less number of gradient

DOI: 10.1002/rnc

experiments compared with the conventional IFT methods for nonlinear systems [16, 17, 15]. It optimizes arbitrary parameters contained in the Hamiltonian function by requiring only two gradient experiments per one step optimization. Third, we also provide a method to directly optimize the elements of the dissipation matrix. One possible important parameter, which does not directly appear in the Hamiltonian function, is the dissipation coefficient appearing as the dissipation matrix of the system. For example, the D feedback gain in the PD controller for a mechanical system corresponds to the case, and thus it was not directly optimized in the early version of this paper [23]. The present paper provides a solution to this issue in the case of mechanical systems by equipping a dynamic feedback of the generalized coordinate instead of the corresponding static feedback of the generalized velocity. We show that the resultant system with the dynamic feedback and a coordinate transformation is represented another Hamiltonian system, and moreover that the dissipation coefficient directly appears in the new Hamiltonian function of the system. Therefore, it can be optimized by the proposed IFT method. Forth, we explicitly deal with parameter constraints. Tuning parameters should often be optimized within prescribed search ranges. We provide an IFT algorithm considering constraints on the parameter search range by adapting the idea of ILC method with input saturation technique in [21]. This practically useful feature is also new from our previous report [23]. Finally, to demonstrate the effectiveness of the proposed method, numerical simulations of a two-link robot manipulator are executed, where the total number of the required experiments and optimization performance between the proposed method and the conventional IFT methods are compared.

As additional distinguished features of the proposed IFT method, it can optimize not only feedback gains aimed in the conventional IFT methods, but also other adjustable parameters, for example, parameters of the plant system itself such as the mass, inertia, link length, stiffness and so on, since they appear in the Hamiltonian function. Also, since the proposed IFT has affinity to the ILC method [20, 21], it can be applied to simultaneous learning control with IFT and ILC. Applications to those directions have been reported in [22, 24].

Finally, let us summarize the main contributions and features of the proposed method in this paper.

- A novel IFT method for a Hamiltonian system is proposed, which utilizes a special property of Hamiltonian systems called variational symmetry in the gradient calculation. The proposed IFT is executed by only using input-output data without model identification;
- Although a Hamiltonian system is a class of nonlinear systems, the proposed method requires only two gradient experiments per one step optimization for any number of parameters contained in the Hamiltonian and the dissipation matrix; and
- The proposed method deals with range constraints on the tuning parameters by adapting the input saturation to the associated input-output relation with the variational symmetry. The parameters are optimized within prescribed search ranges.

2. PRELIMINARIES

This section briefly refers to preliminary backgrounds.

Prepared using rncauth.cls
DOI: 10.1002/rnc

2.1. Variational symmetry of Hamiltonian systems

Our plant is a Hamiltonian system with dissipation $\Sigma^{x_{t^0}}$ with a controlled Hamiltonian $H(x,u)$ as $\Sigma^{x_{t^0}} : U \to Y : u \mapsto y$:

$$\left\{ \begin{array}{rcll} \dot{x} & = & (J-R)\dfrac{\partial H(x,u)}{\partial x}^\top, & x(t^0) = x_{t^0} \\ y & = & -\dfrac{\partial H(x,u)}{\partial u}^\top & \end{array} \right. . \tag{1}$$

Here, $x(t) \in X$ denotes the state, and $u \in U$ and $y \in Y$ represent the input and the output, respectively, where Hilbert spaces X, U and Y are $X = \mathbb{R}^n$, $U, Y = L_2^m[t^0, t^1]$. In this paper, we consider the behaviors of the system (1) on a finite time interval $[t^0, t^1]$. The structure matrix $J \in \mathbb{R}^{n\times n}$ and the dissipation matrix $R \in \mathbb{R}^{n\times n}$ are skew-symmetric and symmetric positive semi-definite, respectively. The matrix R represents dissipative elements such as friction of mechanical systems and resistance of electric circuits.

For this system, let us refer to the following lemma.

Lemma 1

([20]) Consider the Hamiltonian system $\Sigma^{x_{t^0}}$ in (1). The Fréchet derivative $(\delta\Sigma^{x_{t^0}}(u))(\cdot)$ of $\Sigma^{x_{t^0}}(u)$ is called the variational system, and is described by another linear Hamiltonian system with $x_v \in X$, $u_v \in U$ and $y_v \in Y$ as

$$y_v = (\delta\Sigma^{x_{t^0}}(u))(u_v) : \left\{ \begin{array}{rcll} \dot{x} & = & (J-R)\dfrac{\partial H(x,u)}{\partial x}^\top, & x(t^0) = x_{t^0} \\ \dot{x}_v & = & (J-R)\dfrac{\partial H_v(x,u,x_v,u_v)}{\partial x_v}^\top, & x_v(t^0) = 0 \\ y_v & = & -\dfrac{\partial H_v(x,u,x_v,u_v)}{\partial u_v}^\top & \end{array} \right. , \tag{2}$$

where the controlled Hamiltonian $H_v(x,u,x_v,u_v)$ is given by

$$H_v(x,u,x_v,u_v) = \frac{1}{2}\begin{pmatrix} x_v \\ u_v \end{pmatrix}^\top \frac{\partial^2 H(x,u)}{\partial (x,u)^2}\begin{pmatrix} x_v \\ u_v \end{pmatrix}.$$

The adjoint operator plays an important role in solving optimal control problems [25]. According to [26, 20], the adjoint system of the variational system, called the variational adjoint system, is defined by

$$y_a = (\delta\Sigma^{x_{t^0}}(u))^*(u_a) : \left\{ \begin{array}{rcl} \dot{x} & = & (J-R)\dfrac{\partial H(x,u)}{\partial x}^\top, \quad x(t^0) = x_{t^0} \\ \begin{pmatrix} \dot{x}_a \\ y_a \end{pmatrix} & = & \begin{pmatrix} -I_n & 0_{n\times n} \\ 0_{n\times n} & I_n \end{pmatrix}\left(\begin{pmatrix} J-R & 0_{n\times n} \\ 0_{n\times n} & -I_n \end{pmatrix}\dfrac{\partial^2 H(x,u)}{\partial (x,u)^2}\right)^\top \begin{pmatrix} x_a \\ u_a \end{pmatrix}, \\ x_a(t^1) & = & 0, \end{array} \right. \tag{3}$$

DOI: 10.1002/rnc

where $x_a \in X$, $u_a \in Y$ and $y_a \in U$, and I_i and $0_{i\times j}$ denote the $i \times i$ identity matrix and the $i \times j$ zero matrix, respectively.

Then, the following theorem holds between the variational and its adjoint systems of a Hamiltonian system. This property is called variational symmetry of Hamiltonian systems.

Theorem 1

([20]) Consider the Hamiltonian system (1). Suppose that $J - R$ is nonsingular and that there exists a nonsingular matrix $T \in \mathbb{R}^{n\times n}$ satisfying

$$J = -TJT^{-1}, \qquad R = TRT^{-1} \tag{4}$$

$$\frac{\partial^2 H(x,u)}{\partial(x,u)^2} = \begin{pmatrix} T & 0_{n\times n} \\ 0_{n\times n} & I_n \end{pmatrix} \frac{\partial^2 H(x,u)}{\partial(x,u)^2} \begin{pmatrix} T^{-1} & 0_{n\times n} \\ 0_{n\times n} & I_n \end{pmatrix}. \tag{5}$$

Then, a state-space realization of the variational adjoint system (3) coincides with a time-reversal version of that of the variational system (2), namely,

$$y_a = (\delta\Sigma^{x_{t^0}}(u))^*(u_a) : \begin{cases} \dot{x} = (J-R)\dfrac{\partial H(x,u)}{\partial x}^\top, \quad x(t^0) = x_{t^0} \\ \dot{\bar{x}}_v = -(J-R)\dfrac{\partial H_v(x,u,\bar{x}_v,u_a)}{\partial \bar{x}_v}^\top, \\ \bar{x}_v(t^1) = 0 \\ y_a = -\dfrac{\partial H_v(x,u,\bar{x}_v,u_a)}{\partial u_a}^\top \end{cases}. \tag{6}$$

Regarding the variational symmetry, the following theorem is useful.

Theorem 2

([20]) Consider the Hamiltonian system (1) and suppose that conditions of Theorem 1 are satisfied. Suppose moreover that, for two inputs $v, w \in U$, the corresponding state trajectories $\phi(t), \psi(t) \in X, t \in [t^0, t^1]$ satisfy

$$\mathcal{R}\left(\left.\frac{\partial^2 H(x,u)}{\partial(x,u)^2}\right|_{\substack{x\equiv\phi \\ u\equiv v}} \right) = \left.\frac{\partial^2 H(x,u)}{\partial(x,u)^2}\right|_{\substack{x\equiv\psi \\ u\equiv w}}, \tag{7}$$

where $\mathcal{R}$ represents the time-reversal operator on $[t^0, t^1]$ defined by

$$\mathcal{R}(u)(t) = u(t^1 - t + t^0), \quad \forall t \in [t^0, t^1]. \tag{8}$$

Then, the following relationship holds:

$$(\delta\Sigma^{\phi(t^0)}(v))^* = \mathcal{R} \circ (\delta\Sigma^{\psi(t^0)}(w)) \circ \mathcal{R}. \tag{9}$$

DOI: 10.1002/rnc

3. ITERATIVE FEEDBACK TUNING BASED ON MODIFIED VARIATIONAL SYMMETRY

In this section, we propose a new IFT method based on variational symmetry of Hamiltonian systems. Whereas ILC produces an optimal feedforward input based on the I/O data of experiments, IFT is an algorithm to adjust finite number of parameters of a feedback controller. Since the number of parameters are finite, we can construct a learning algorithm based on the gradient method in which a set of data for a finite number of experiments is required to update the estimation for the parameters. In the conventional IFT methods for nonlinear systems, e.g., [15, 16, 17], the estimation of the gradient of a given cost function needs $s+1$ experiments, where s denotes the number of parameters to be tuned. On the contrary, the proposed method based on variational symmetry has the following significant advantages. First, it requires only 3 experiments to estimate the gradient for any number of parameters to be tuned. Second, since it deals with any parameter contained in the Hamiltonian function, it can optimize not only feedback gains aimed in the conventional IFT methods, but also other adjustable parameters, for example, parameters of the plant itself such as the mass, inertia, link length and/or joint stiffness. We refer to [22, 24] for applications of robot parameter optimization.

3.1. Modified variational symmetry for optimization of finite number of parameters

Let us consider a feedback system of a Hamiltonian system with a generalized canonical transformation [27, 3]. Since a generalized canonical transformation is a set of feedback and coordinate transformations preserving the Hamiltonian structure in Eq. (1), the feedback system has the form of (1) as well. Therefore, the system parameters of the closed-loop system $H(x,u)$, J and R depend on the the parameters of the feedback controller to be adjusted. For simplicity, let us suppose that only the Hamiltonian function $H(x,u)$ depends on the tuning parameter $\rho \in \mathbb{R}^s$. The case where the other system parameters J and R also depend on the tuning parameter will be considered later.

Consider a feedback system (1) with a Hamiltonian $H(x,u,\rho)$ where $\rho \in \mathbb{R}^s$ denotes a set of tuning parameters. Therefore, the dynamics is written as

$$\dot{x} = (J-R)\frac{\partial H(x,u,\rho)}{\partial x}^\top, \quad x(t^0) = x_{t^0}. \tag{10}$$

For this dynamics, let us construct the following I/O mapping $\Sigma_\rho^{x_{t^0},u} : U_\rho \to Y_\rho : y_\rho = \Sigma_\rho^{x_{t^0},u}(u_\rho)$

$$\begin{cases} \dot{x} &= (J-R)\dfrac{\partial H(x,u,u_\rho)}{\partial x}^\top, \quad x(t^0) = x_{t^0} \\ y_\rho &= -\dfrac{\partial H(x,u,u_\rho)}{\partial u_\rho}^\top \end{cases}$$

with $u_\rho \in U_\rho = L_2^s[t^0,t^1]$ and $y_\rho \in Y_\rho = L_2^s[t^0,t^1]$. Since this map $\Sigma_\rho^{x_{t^0},u}$ is a Hamiltonian system of the form (1), Theorem 2 implies that it has variational symmetry, that is, the following relation holds:

$$(\delta\Sigma_\rho^{x_{t^0},u}(u_\rho))^* = \mathcal{R} \circ (\delta\Sigma_\rho^{\psi(t^0),w}(w_\rho)) \circ \mathcal{R},$$

DOI: 10.1002/rnc

where $\psi(t^0), w$ and w_ρ are selected so that the condition (7) holds. In order to describe the true dynamics of the closed-loop system, we need to select $u_\rho \in U_\rho$ as constant with respect to time. To this end, let us introduce a Zero-th order hold operator

$$\mathfrak{h} : \mathbb{R}^s \to U_\rho : (\mathfrak{h}(\rho))(t) \equiv \rho, \ \ \forall t \in [t^0, t^1].$$

Its adjoint $\mathfrak{h}^*$ will be further characterized later in Lemma 2. Then, clearly, the composition map $\Sigma_\rho^{x_{t^0},u} \circ \mathfrak{h}(\rho)$ describe the dynamics in Eq. (10). For this map, let us define the following operator

$$\Sigma_{\mathfrak{h}}^{x_{t^0},u} := \mathfrak{h}^* \circ \Sigma_\rho^{x_{t^0},u} \circ \mathfrak{h} : \mathbb{R}^s \to \mathbb{R}^s. \tag{11}$$

Then, we can prove the modified variational symmetry for the operator $\Sigma_{\mathfrak{h}}^{x_{t^0},u}$.

Theorem 3
Consider the Hamiltonian system (1) and suppose that the conditions (4) and (5) in Theorem 1 and the condition (7) in Theorem 2 hold. Then the following equation holds

$$(\delta\Sigma_{\mathfrak{h}}^{x_{t^0},u}(\rho))^* = \delta\Sigma_{\mathfrak{h}}^{\psi(t^0),w}(\rho). \tag{12}$$

Proof
Proof is obtained from direct calculation. Under the conditions (4), (5) and (7), we have

$$\begin{aligned}
(\delta\Sigma_{\mathfrak{h}}^{x_{t^0},u}(\rho))^* &= (\delta(\mathfrak{h}^* \circ \Sigma_\rho^{x_{t^0},u} \circ \mathfrak{h})(\rho))^* \\
&= (\mathfrak{h}^* \circ \delta\Sigma_\rho^{x_{t^0},u}(\mathfrak{h}(\rho)) \circ \mathfrak{h})^* \\
&= \mathfrak{h}^* \circ (\delta\Sigma_\rho^{x_{t^0},u}(\mathfrak{h}(\rho)))^* \circ \mathfrak{h} \\
&= \mathfrak{h}^* \circ \mathcal{R} \circ (\delta\Sigma_\rho^{\psi(t^0),w}(\mathfrak{h}(\rho))) \circ \mathcal{R} \circ \mathfrak{h} \\
&= \mathfrak{h}^* \circ (\delta\Sigma_\rho^{\psi(t^0),w}(\mathfrak{h}(\rho))) \circ \mathfrak{h} \\
&= \delta(\mathfrak{h}^* \circ \Sigma_\rho^{\psi(t^0),w} \circ \mathfrak{h}(\rho)) \\
&= \delta\Sigma_{\mathfrak{h}}^{\psi(t^0),w}(\rho).
\end{aligned} \tag{13}$$

The second equality in Eq. (13) is derived as follows. It follows from the definition of the Fréchet derivative and linearity of the operator $\mathfrak{h}$ that, for any $\rho_v \in \mathbb{R}^s$,

$$\begin{aligned}
(\delta(\mathfrak{h}^* \circ \Sigma_\rho^{x_{t^0},u} \circ \mathfrak{h})(\rho))(\rho_v) &= \mathfrak{h}^* \circ \Sigma_\rho^{x_{t^0},u} \circ \mathfrak{h}(\rho + \rho_v) - \mathfrak{h}^* \circ \Sigma_\rho^{x_{t^0},u} \circ \mathfrak{h}(\rho) + o(\|\rho_v\|_{\mathbb{R}^s}) \\
&= \mathfrak{h}^* \circ \Sigma_\rho^{x_{t^0},u}(\mathfrak{h}(\rho) + \mathfrak{h}(\rho_v)) - \mathfrak{h}^* \circ \Sigma_\rho^{x_{t^0},u}(\mathfrak{h}(\rho)) + o(\|\mathfrak{h}(\rho_v)\|_{U_\rho}) \\
&= \mathfrak{h}^* \circ (\delta\Sigma_\rho^{x_{t^0},u}(\mathfrak{h}(\rho)))(\mathfrak{h}(\rho_v)) \\
&= \mathfrak{h}^* \circ \delta\Sigma_\rho^{x_{t^0},u}(\mathfrak{h}(\rho)) \circ \mathfrak{h}(\rho_v).
\end{aligned}$$

The fourth equality follows from variational symmetry of the system $\Sigma_\rho^{x_{t^0},u}$, and the fifth one is implied by

$$\begin{aligned}
\mathcal{R} \circ \mathfrak{h} &= \mathfrak{h} \\
\mathfrak{h}^* \circ \mathcal{R} &= \mathfrak{h}^* \circ \mathcal{R}^* = (\mathcal{R} \circ \mathfrak{h})^* = \mathfrak{h}^*,
\end{aligned}$$

DOI: 10.1002/rnc

where note that it follows from Eq. (8) that $R^* = R$. This proves the theorem. □

As in the previous result shown in Theorem 2, we call the resultant property (12) in Theorem 3 a modified variational symmetry for IFT, which will play a fundamental role in the proposed IFT method. Here, let us explain the significance and necessity of the modified variational symmetry. The original variational symmetry (9) is defined for the I/O mapping on $L_2^m[t^0, t^1]$, and thus it cannot be used for IFT, since ρ is a constant vector on $\mathbb{R}^s$. Thus, we first introduce a virtual I/O mapping $\Sigma_\rho^{x_{t^0},u}$ on $L_2^s[t^0, t^1]$ using the Zero-th order hold operator $\mathfrak{h}$ from ρ, which can enjoy the original variational symmetry. However, this is still insufficient to apply to IFT. Since even if u_ρ is constant during $[t^0, t^1]$, its variational input is not necessarily constant. This results in that the resultant iteration law for the gradient experiment becomes time-varying, which cannot be used for the constant parameter update. To solve this issue and to properly adapt to IFT, this paper newly defines the mapping $\Sigma_\mathfrak{h}^{x_{t^0},u}$ in (11), and derives another version of the variational symmetry for $\Sigma_\mathfrak{h}$ in Theorem 3 using the properties of $\mathfrak{h}$ and $\mathfrak{h}^*$. This result finally enables to lead the new IFT iteration law for the parameter optimization as will presented in the next subsection.

3.2. Derivation of the iteration law for the proposed IFT

This subsection derives the iteration law for the proposed IFT based on the modified variational symmetry characterized in Theorem 3. Before stating the result, the following property is exhibited.

Lemma 2
$\mathfrak{h}^*$ is characterized by the following equation with any $y_\rho \in L_2^s[t^0, t^1]$.

$$\mathfrak{h}^*(y_\rho) = \int_{t^0}^{t^1} y_\rho(t)\mathrm{d}t.$$

Proof
The adjoint $\mathfrak{h}^*$ satisfies the following equations for arbitrary $\rho \in \mathbb{R}^s$ and $y_\rho \in L_2^s[t^0, t^1]$:

$$\begin{aligned}\langle \mathfrak{h}^*(y_\rho), \rho\rangle_{\mathbb{R}^s} &= \langle y_\rho, \mathfrak{h}(\rho)\rangle_{L_2^s[t^0,t^1]} \\ &= \int_{t^0}^{t^1} \rho^\top y_\rho(t)\mathrm{d}t \\ &= \left\langle \int_{t^0}^{t^1} y_\rho(t)\mathrm{d}t, \rho \right\rangle_{\mathbb{R}^s}.\end{aligned}$$

Since the above equation holds for arbitrary ρ and y_ρ, the lemma is true. □

The investigation given in Subsection 3.1 derives that any cost function of the input and output of the operator $\Sigma_\mathfrak{h}^{x_{t^0},u}$ can be minimized by only using I/O data as in the ILC case.

DOI: 10.1002/rnc

Theorem 3 and Lemma 2 imply that the closed-loop system (10) should be rewritten by $\Sigma_{\mathfrak{h}}^{x_{t^0},u}(\rho):\mathbb{R}^s\to\mathbb{R}^s$ as

$$\eta=\Sigma_{\mathfrak{h}}^{x_{t^0},u}(\rho):\left\{\begin{array}{rcl}\dot{x}&=&(J-R)\dfrac{\partial H(x,u,\rho)}{\partial x}^{\top},\\ x(t^0)&=&x_{t^0}\\ \\ \eta&=&-\displaystyle\int_{t^0}^{t^1}\frac{\partial H(x,u,\rho)}{\partial\rho}^{\top}\mathrm{d}t\end{array}\right.. \tag{14}$$

In order to utilize Theorem 3 for IFT, the cost function to be minimized should have a form $\hat{\Gamma}(\rho,\eta):\mathbb{R}^s\times\mathbb{R}^s\to\mathbb{R}$. Under the relation $\eta=\Sigma_{\mathfrak{h}}^{x_{t^0},u}(\rho)$ in (14), the gradient of the cost function $\Gamma(\rho):=\hat{\Gamma}(\rho,\Sigma_{\mathfrak{h}}^{x_{t^0},u}(\rho))$ with respect to ρ, denoted by $\nabla\Gamma(\rho)$, is given as follows:

$$\begin{aligned}\langle\nabla\Gamma(\rho),\mathrm{d}\rho\rangle_{\mathbb{R}^s}&=\langle\nabla_\rho\hat{\Gamma}(\rho,\eta),\ \mathrm{d}\rho\rangle_{\mathbb{R}^s}+\langle\nabla_\eta\hat{\Gamma}(\rho,\eta),\ \mathrm{d}\eta\rangle_{\mathbb{R}^s}\\&=\langle\nabla_\rho\hat{\Gamma}(\rho,\eta)+(\delta\Sigma_{\mathfrak{h}}^{x_{t^0},u}(\rho))^*(\nabla_\eta\hat{\Gamma}(\rho,\eta)),\ \mathrm{d}\rho\rangle_{\mathbb{R}^s},\end{aligned} \tag{15}$$

where $\nabla_\rho\hat{\Gamma}(\rho,\eta)$ and $\nabla_\eta\hat{\Gamma}(\rho,\eta)$ denote the partial gradients, and they can be obtained by experiments. Then, the gradient $\nabla\Gamma(\rho)$ in Eq. (15), all terms except the variational adjoint $(\delta\Sigma_{\mathfrak{h}}^{x_{t^0},u}(\rho))^*$ are known. In this way, we need to construct a variational adjoint of the plant system in order to estimate the gradient of the cost function. However, since the construction of the variational adjoint for a general nonlinear system requires the precise knowledge of the plant system, we utilize the variational symmetry. Theorem 3 implies that the gradient $\nabla\Gamma(\rho)$ in (15) is given by

$$\begin{aligned}\nabla\Gamma(\rho)&=\nabla_\rho\hat{\Gamma}(\rho,\eta)+(\delta\Sigma_{\mathfrak{h}}^{x_{t^0},u}(\rho))^*(\nabla_\eta\hat{\Gamma}(\rho,\eta))\\&=\nabla_\rho\hat{\Gamma}(\rho,\eta)+(\delta\Sigma_{\mathfrak{h}}^{\psi(t^0),w}(\rho))(\nabla_\eta\hat{\Gamma}(\rho,\eta)),\end{aligned} \tag{16}$$

Further, due to the Fréchet derivative, the variational system $\delta\Sigma_{\mathfrak{h}}^{\psi(t^0),w}(\rho)$ can be approximated by

$$(\delta\Sigma_{\mathfrak{h}}^{\psi(t^0),w}(\rho))(\nu)=\frac{1}{\epsilon}(\delta\Sigma_{\mathfrak{h}}^{\psi(t^0),w}(\rho))(\epsilon\nu)=\frac{1}{\epsilon}\left(\Sigma_{\mathfrak{h}}^{\psi(t^0),w}(\rho+\epsilon\nu)-\Sigma_{\mathfrak{h}}^{\psi(t^0),w}(\rho)\right)+\frac{o(\epsilon)}{\epsilon}, \tag{17}$$

where ϵ represents the tolerance of the approximation, and $o(\cdot)$ denotes a term satisfying $\lim_{\epsilon\to0}o(\epsilon)/\epsilon=0$.

Once we can obtain the gradient estimation for the cost function $\hat{\Gamma}(\rho,\eta)$ based on Eqs. (16) and (17), we provide the following parameter update law according to the gradient method:

$$\begin{aligned}&\rho_{(i+1)}=\rho_{(i)}-K_{\rho(i)}\nabla\Gamma(\rho_{(i)})\\&=\rho_{(i)}-K_{\rho(i)}\left(\nabla_\rho\hat{\Gamma}(\rho_{(i)},\eta_{(i)})+\left(\delta\Sigma_{\mathfrak{h}}^{\psi_{(i)}(t^0),w_{(i)}}(\rho_{(i)})\right)(\nabla_\eta\hat{\Gamma}(\rho_{(i)},\eta_{(i)}))\right)\\&\approx\rho_{(i)}-K_{\rho(i)}\left(\nabla_\rho\hat{\Gamma}(\rho_{(i)},\eta_{(i)})+\frac{1}{\epsilon_{(i)}}\left(\Sigma_{\mathfrak{h}}^{\psi_{(i)}(t^0),w_{(i)}}(\rho_{(i)}+\epsilon_{(i)}\nabla_\eta\hat{\Gamma}(\rho_{(i)},\eta_{(i)}))-\Sigma_{\mathfrak{h}}^{\psi_{(i)}(t^0),w_{(i)}}(\rho_{(i)})\right)\right),\end{aligned} \tag{18}$$

where a positive definite matrix $K_{\rho(i)}$ denotes the step parameter of the gradient method and the subscript $(\cdot)_{(i)}$ denotes the data in the ith step of iteration. In each step, we need two more

DOI: 10.1002/rnc

experiments in order to produce the I/O mapping of the operator $\Sigma_{\mathfrak{h}}^{\psi_{(i)}(t^0),w_{(i)}}$. Therefore, the iteration law of IFT is given by

$$\begin{cases} x_{t^0(3i+1)} &= \psi_{(i)}(t^0) \\ u_{(3i+1)} &= w_{(i)} \\ \rho_{(3i+1)} &= \rho_{(3i)} \end{cases}$$
$$\begin{cases} x_{t^0(3i+2)} &= \psi_{(i)}(t^0) \\ u_{(3i+2)} &= w_{(i)} \\ \rho_{(3i+2)} &= \rho_{(3i)} + \epsilon_{(i)} \nabla_\eta \hat{\Gamma}(\rho_{(3i)}, \eta_{(3i)}) \end{cases} \tag{19}$$
$$\begin{cases} x_{t^0(3i+3)} &= x_{t^0} \\ u_{(3i+3)} &\equiv 0_{m\times 1} \\ \rho_{(3i+3)} &= \rho_{(3i)} - K_{\rho(i)} \left(\nabla_\rho \hat{\Gamma}(\rho_{(3i)}, \eta_{(3i)}) + \frac{1}{\epsilon_{(i)}} (\eta_{(3i+2)} - \eta_{(3i+1)}) \right) \end{cases} .$$

Here, $\epsilon_{(i)}$ represents the tolerance of the difference approximation (17) at the ith iteration. Besides, $\psi_{(i)}(t^0)$ and $w_{(i)}$ are chosen such that the condition (7) is satisfied with the trajectory derived by the pair of $x_{t^0(3i)}$ and $u_{(3i)}$ with $\rho_{(3i)}$. How to select $\psi_{(i)}(t^0)$ and $w_{(i)}$ is discussed in [21], and a concrete iteration procedure will be given for mechanical systems in the next section.

3.3. Parameter constraints using input saturation technique

Adjustable parameters should often be optimized within a prescribed search range. Thus, this subsection provides a modified iteration law considering constraints on the parameter search range. The literature [21] proposes an ILC method dealing with input saturation. We adapt this idea to the proposed IFT method in the previous subsection. Compared to the conventional IFT methods, this method guarantees that the parameters are optimized within prescribed ranges.

We suppose that the parameter constraints are characterized by

$$\rho = \alpha(\hat{\rho}), \tag{20}$$

where $\hat{\rho}$ denotes the command parameter and ρ means the actual parameter to the system. The saturation function is supposed to be differentiable and given. By assigning appropriate saturation functions, we can optimize the adjustable parameters within the prescribed ranges. We will show some possibilities of the saturation function later. Now, we derive the iteration law for IFT considering input constraints (20). We consider a cost function to be minimized as $\hat{\Gamma}(\hat{\rho}, \eta) : \mathbb{R}^s \times \mathbb{R}^s \to \mathbb{R}$. The Fréchet derivative of the cost function is given by

$$\begin{aligned} \delta\hat{\Gamma}(\hat{\rho},\eta)(\mathrm{d}\hat{\rho},\mathrm{d}\eta) &= \langle \nabla_{\hat{\rho}}\hat{\Gamma}(\hat{\rho},\eta), \mathrm{d}\hat{\rho}\rangle_{\mathbb{R}^s} + \langle \nabla_\eta \hat{\Gamma}(\hat{\rho},\eta), \mathrm{d}\eta\rangle_{\mathbb{R}^s} \\ &= \langle \nabla_{\hat{\rho}}\hat{\Gamma}, \mathrm{d}\hat{\rho}\rangle_{\mathbb{R}^s} + \langle (\delta\Sigma_{\mathfrak{h}}^{x_{t^0},u}(\rho))^*(\nabla_\eta\hat{\Gamma}), \mathrm{d}\rho\rangle_{\mathbb{R}^s} \\ &= \langle \nabla_{\hat{\rho}}\hat{\Gamma}, \mathrm{d}\hat{\rho}\rangle_{\mathbb{R}^s} + \left\langle (\delta\Sigma_{\mathfrak{h}}^{x_{t^0},u}(\rho))^*(\nabla_\eta\hat{\Gamma}), \frac{\partial\alpha(\hat{\rho})}{\partial\hat{\rho}}\,\mathrm{d}\hat{\rho} \right\rangle_{\mathbb{R}^s} \\ &= \left\langle \nabla_{\hat{\rho}}\hat{\Gamma} + \frac{\partial\alpha(\hat{\rho})}{\partial\hat{\rho}}^\top (\delta\Sigma_{\mathfrak{h}}^{x_{t^0},u}(\rho))^*(\nabla_\eta\hat{\Gamma}), \mathrm{d}\hat{\rho} \right\rangle_{\mathbb{R}^s} . \end{aligned} \tag{21}$$

DOI: 10.1002/rnc

By adapting similar calculation with Eqs. (17) and (18) to Eq. (21), we obtain the modified iteration law of IFT considering parameter constraints as

$$
\begin{cases} x_{t^0(3i+1)} &= \psi_{(i)}(t^0) \\ u_{(3i+1)} &= w_{(i)} \\ \rho_{(3i+1)} &= \alpha(\hat{\rho}_{(3i)}) \end{cases}
\begin{cases} x_{t^0(3i+2)} &= \psi_{(i)}(t^0) \\ u_{(3i+2)} &= w_{(i)} \\ \rho_{(3i+2)} &= \rho_{(3i)} + \epsilon_{(i)} \nabla_\eta \hat{\Gamma}(\hat{\rho}_{(3i)}, \eta_{(3i)}) \end{cases}
\begin{cases} x_{t^0(3i+3)} &= x_{t^0} \\ u_{(3i+3)} &\equiv 0_{m\times 1} \\ \rho_{(3i+3)} &= \alpha\left(\hat{\rho}_{(3i)} - K_{\rho(i)}\left(\nabla_{\hat{\rho}}\hat{\Gamma}(\hat{\rho}_{(3i)}, \eta_{(3i)}) + \frac{1}{\epsilon_{(i)}}\frac{\partial \alpha(\hat{\rho}_{(3i)})}{\partial \hat{\rho}}^\top (\eta_{(3i+2)} - \eta_{(3i+1)})\right)\right) \end{cases}. \tag{22}
$$

4. APPLICATION TO MECHANICAL SYSTEMS

This section considers application of IFT method proposed in the previous section to mechanical systems. It provides concrete procedures including construction of $\psi(t^0)$ and w in Theorem 2. We also provide a method to optimize the elements of the dissipation matrix, which do not directly appear in the Hamiltonian, by using a filtered derivative.

Let us consider the following typical mechanical system of the form (1), which includes the robot manipulator dynamics:

$$
\begin{pmatrix} \dot{q} \\ \dot{p} \end{pmatrix} = \left(\begin{pmatrix} 0_{m\times m} & I_m \\ -I_m & 0_{m\times m} \end{pmatrix} - \begin{pmatrix} 0_{m\times m} & 0_{m\times m} \\ 0_{m\times m} & R_D \end{pmatrix} \right) \begin{pmatrix} \frac{\partial H(q,p,u)}{\partial q}^\top \\ \frac{\partial H(q,p,u)}{\partial p}^\top \end{pmatrix} \tag{23}
$$

with the Hamiltonian

$$
H(q,p,u) = \frac{1}{2} p^\top M(q)^{-1} p + U(q) - u^\top q. \tag{24}
$$

The state is defined as $x := (q^\top, p^\top)^\top \in \mathbb{R}^{2m}$. A positive definite matrix $M(q) \in \mathbb{R}^{m\times m}$ denotes the inertia matrix. The generalized momentum $p \in \mathbb{R}^m$ is given by $p := M(q)\dot{q}$. A positive semi-definite matrix $R_D \in \mathbb{R}^{m\times m}$ denotes the friction coefficients, and a scalar function $U(q) \in \mathbb{R}$ denotes the potential energy of the system.

Here, we consider a PD controller as a practically important class of the feedback controller for a mechanical system. It is known that the PD feedback renders the mechanical system of (23) asymptotically stable, and moreover it preserves the Hamiltonian structure of the closed-loop system [27, 20]. A general class of feedback controller design preserving the Hamiltonian structure of the closed-loop system is formulated in the literature [27, 2], and the proposed method is applicable to the general class of controllers as well. Let us consider a PD controller

$$
u = -K_P q - K_D \dot{q} + \bar{u}, \tag{25}
$$

DOI: 10.1002/rnc

where $\bar{u}$ is a new input and $K_P, K_D \in \mathbb{R}^{m\times m}$ are symmetric positive definite matrices, respectively. The closed-loop system of (23) with the PD controller (25) is again described as the form of (1), where

$$J = \begin{pmatrix} 0_{m\times m} & I_m \\ -I_m & 0_{m\times m} \end{pmatrix}, \quad R = \begin{pmatrix} 0_{m\times m} & 0_{m\times m} \\ 0_{m\times m} & R_D + K_D \end{pmatrix} \tag{26}$$

with the Hamiltonian

$$H(q,p,\bar{u}) = \frac{1}{2}p^\top M(q)^{-1}p + U(q) + \frac{1}{2}q^\top K_P q - \bar{u}^\top q. \tag{27}$$

The feedback system is depicted in Fig. 1.

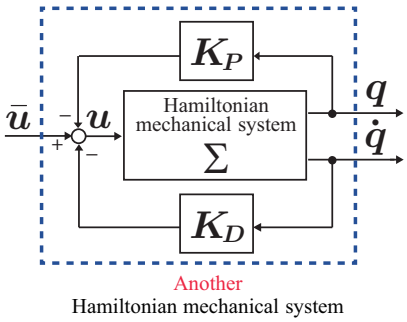

Figure 1. PD feedback system

In considering the P feedback gain K_P and the D feedback gain K_D in Eq. (25) to be optimized by the proposed method, there is an issue that K_P is contained in the Hamiltonian in the closed-loop system (27), while K_D appears as an element of the dissipation matrix of the closed-loop system as in Eq. (26), and thus it does not appear in the Hamiltonian. Therefore, the proposed method mentioned in Section 3 cannot be directly applied to the D feedback gain K_D. To overcome this issue, we provide a solution method using a filtered derivative. Now, we consider the following practical PD controller [28, 29] instead of Eq. (25):

$$\mathcal{L}[u] = -K_P\mathcal{L}[q] - K_D\frac{s}{\tau s+1}\mathcal{L}[q] + \mathcal{L}[\bar{u}], \tag{28}$$

where $\mathcal{L}[\cdot]$ denotes the Laplace transform. A positive constant τ in the attached low-pass filter in Eq. (28) specifies the effective band of the derivative term. Figure 2 shows the Bode diagram of the filtered derivative operators, where τ changes to $0.01, 0.1$ and 1, respectively. The exact derivative operator in PD controller has an implementation issue that it has high-frequency amplification, and thus the high-frequency measurement noise is amplified [28, 29]. Since the filtered derivative with appropriate effective band behaves as the exact derivative in the effective domain, and its high-frequency gain is saturated (see, Fig. 2), the practical PD controller (28) is well utilized instead of the exact PD controller (25). The state space representation of the filtered derivative

DOI: 10.1002/rnc

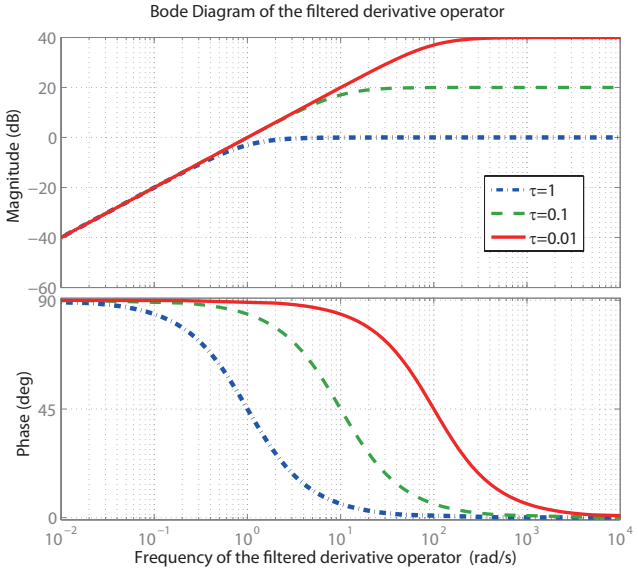

Figure 2. Bode diagram of the filtered derivative operators with $\tau = 0.01, 0.1$ and 1

$\mathcal{L}[y_\sigma] = s/(\tau s + 1)\mathcal{L}[u_\sigma]$ is given by

$$\begin{aligned} \dot{\sigma} &= -\frac{1}{\tau}\sigma - \frac{1}{\tau^2}u_\sigma \\ y_\sigma &= \sigma + \frac{1}{\tau}u_\sigma \end{aligned} \tag{29}$$

with the state variable σ. Thus, from Eqs. (23), (28) and (29), it is found that the closed-loop system of (23) with the practical PD controller with filtered derivative in (28) is described by the following Hamiltonian representation:

$$\begin{pmatrix} \dot{q} \\ \dot{p} \\ \dot{\sigma} \end{pmatrix} = \begin{pmatrix} 0_{m\times m} & I_m & 0_{m\times m} \\ -I_m & -R_D & 0_{m\times m} \\ 0_{m\times m} & 0_{m\times m} & -\frac{{K_D}^{-1}}{\tau^2} \end{pmatrix} \begin{pmatrix} \frac{\partial \bar{H}(q,p,\sigma,\bar{u})}{\partial q}^\top \\ \frac{\partial \bar{H}(q,p,\sigma,\bar{u})}{\partial p}^\top \\ \frac{\partial \bar{H}(q,p,\sigma,\bar{u})}{\partial \sigma}^\top \end{pmatrix} \tag{30}$$

with the new Hamiltonian

$$\begin{aligned} \bar{H}(q,p,\sigma,\bar{u}) &= \frac{1}{2}p^\top M(q)^{-1}p + U(q) + \frac{1}{2}q^\top K_P q + q^\top K_D \sigma + \frac{\tau}{2}\sigma^\top K_D \sigma + \frac{1}{2\tau}q^\top K_D q - \bar{u}^\top q \\ &= \frac{1}{2}p^\top M(q)^{-1}p + U(q) + \frac{1}{2}q^\top K_P q + \frac{\tau}{2}\left(\sigma + \frac{q}{\tau}\right)^\top K_D \left(\sigma + \frac{q}{\tau}\right) - \bar{u}^\top q. \end{aligned} \tag{31}$$

The closed-loop system is depicted in Fig. 3. Compared with the case of the system (23) with the exact PD controller (25), both the P gain K_p and the D gain K_D explicitly appear in the Hamiltonian (31) in the case of the system (23) with the practical PD controller (28). However, since K_D appears not only in the Hamiltonian (31), but also in the dissipation matrix of the system dynamics in (30),

DOI: 10.1002/rnc

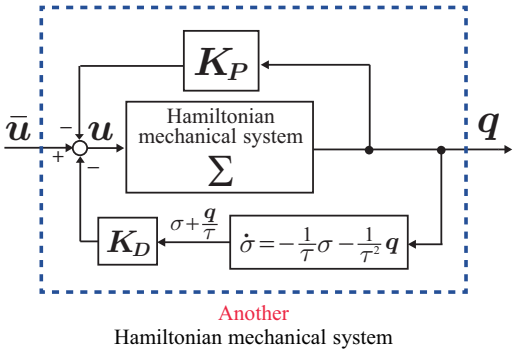

Figure 3. Closed-loop system with the practical PD feedback

as ${K_D}^{-1}/\tau^2$, we further consider the following coordinate transformation:

$$\bar{\sigma} := \tau {K_D}^{\frac{1}{2}}. \tag{32}$$

By applying the coordinate transformation (32), the system (23) is converted as

$$\begin{pmatrix} \dot{q} \\ \dot{p} \\ \dot{\bar{\sigma}} \end{pmatrix} = \begin{pmatrix} 0_{m\times m} & I_m & 0_{m\times m} \\ -I_m & -R_D & 0_{m\times m} \\ 0_{m\times m} & 0_{m\times m} & -I_m \end{pmatrix} \begin{pmatrix} \frac{\partial \mathcal{H}(q,p,\bar{\sigma},\bar{u})}{\partial q}^\top \\ \frac{\partial \mathcal{H}(q,p,\bar{\sigma},\bar{u})}{\partial p}^\top \\ \frac{\partial \mathcal{H}(q,p,\bar{\sigma},\bar{u})}{\partial \bar{\sigma}}^\top \end{pmatrix} \tag{33}$$

with the new Hamiltonian

$$\begin{aligned} \mathcal{H}(q,p,\bar{\sigma},\bar{u}) &= \frac{1}{2}p^\top M(q)^{-1}p + U(q) + \frac{1}{2}q^\top K_P q + \frac{1}{2\tau}\bar{\sigma}^\top\bar{\sigma} + \frac{1}{\tau}q^\top {K_D}^{\frac{1}{2}}\bar{\sigma} + \frac{1}{2\tau}q^\top K_D q - \bar{u}^\top q \\ &= \frac{1}{2}p^\top M(q)^{-1}p + U(q) + \frac{1}{2}q^\top K_P q + \frac{1}{2\tau}\left({K_D}^{-\frac{1}{2}}\bar{\sigma} + q\right)^\top K_D \left({K_D}^{-\frac{1}{2}}\bar{\sigma} + q\right) - \bar{u}^\top q. \end{aligned} \tag{34}$$

From the resultant system (33) with (34), we can observe that K_D only appears in the Hamiltonian (34). Also, note that this system can satisfy the conditions (4) and (5) of Theorem 1 with the matrix

$$T = \begin{pmatrix} I_m & 0_{m\times m} & 0_{m\times m} \\ 0_{m\times m} & -I_m & 0_{m\times m} \\ 0_{m\times m} & 0_{m\times m} & I_m \end{pmatrix}$$

as in the literature [20]. Therefore, we can apply the IFT method characterized in the previous section. Thus, by considering the system (33) with (34), we can optimize both K_P and K_D with the proposed IFT method.

Finally, note that in the Hamiltonian formulation, the literature [30] provides a Hamiltonian representation of the filtered derivative, and equip this in order to replace a velocity feedback with the dynamic position feedback. The Hamiltonian representation used in this paper in Eqs. (30) and (31) is slightly different from that in [30] that K_D appears in the dissipation matrix of the dynamics and ${K_D}^{-1}$ does in the Hamiltonian in [30]. On the contrary, in our setting with Eqs. (30) and (31), the appearance of ${K_D}^{-1}$ and K_D is reversed, which is convenient for our purpose.

DOI: 10.1002/rnc

Now, let us define $\rho := (\rho_P^\top, \rho_D^\top)^\top \in \mathbb{R}^{m(m+1)}$ with

$$\rho_P := ([K_P]_{1,1}, \ldots, [K_P]_{1,m}, [K_P]_{2,2}, \ldots, [K_P]_{2,m}, \ldots, [K_P]_{m,m})^\top \in \mathbb{R}^{m(m+1)/2} \tag{35}$$

$$\rho_D := ([K_D]_{1,1}, \ldots, [K_D]_{1,m}, [K_D]_{2,2}, \ldots, [K_D]_{2,m}, \ldots, [K_D]_{m,m})^\top \in \mathbb{R}^{m(m+1)/2}, \tag{36}$$

where for a matrix A, $[A]_{i,j}$ denotes its (i,j)th element. From Eq. (34), we have

$$\frac{\partial \mathcal{H}}{\partial [K_P]_{i,j}} = \begin{cases} \dfrac{q_i^2}{2} & i = j \\ q_i q_j & i \neq j \end{cases}, \tag{37}$$

$$\frac{\partial \mathcal{H}}{\partial [K_D]_{i,j}} = \begin{cases} \dfrac{q_i^2}{2\tau} + \displaystyle\sum_{k,l=1}^{m} \frac{1}{\tau} \frac{\partial [K_D{}^{\frac{1}{2}}]_{k,l}}{\partial [K_D]_{i,i}} q_k \bar{\sigma}_l & i = j \\ \dfrac{q_i q_j}{\tau} + \displaystyle\sum_{k,l=1}^{m} \frac{1}{\tau} \frac{\partial [K_D{}^{\frac{1}{2}}]_{k,l}}{\partial [K_D]_{i,j}} q_k \bar{\sigma}_l & i \neq j \end{cases}. \tag{38}$$

Then, by using Eqs. (14), (35), (36), (37) and (38), we can define the corresponding output $\eta := (\eta_P^\top, \eta_D^\top)^\top \in \mathbb{R}^{m(m+1)}$ with

$$\eta_P = -\int_{t^0}^{t^1} \frac{\partial \mathcal{H}}{\partial \rho_P}^\top \mathrm{d}t$$

$$\eta_D = -\int_{t^0}^{t^1} \frac{\partial \mathcal{H}}{\partial \rho_D}^\top \mathrm{d}t.$$

In a similar manner, we can choose any adjustable parameter contained in the Hamiltonian to be ρ. Once ρ is determined, the corresponding output η is defined by Eq. (14).

In order to produce the trajectory of $\delta\Sigma_{\mathfrak{h}}^{\psi(t^0),w}$ satisfying the condition (7), we select the reference signals as

$$\begin{aligned} q^r &= \mathcal{R}(q_{old}) \\ \dot{q}^r &= -\mathcal{R}(\dot{q}_{old}) \end{aligned}$$

with the initial states

$$\begin{aligned} q^r(t^0) &= q_{old}(t^1) \\ \dot{q}^r(t^0) &= -\dot{q}_{old}(t^1), \end{aligned}$$

where q_{old} and $\dot{q}_{old}$ denote the data q and $\dot{q}$ in the previous step of iteration. That is, they are selected such that the two state trajectories $x = (q,p)$ and $x_{old} = (q_{old}, p_{old})$ satisfy the condition (7) for variational symmetry. A simple way to track the reference signals $(q^r, \dot{q}^r)$, we can regard that the input $\bar{u} = w$ is selected as a PD controller:

$$\begin{aligned} \bar{u} = w &= L_P(q - q^r) + L_D(\dot{q} - \dot{q}^r) \\ &= L_P(q - \mathcal{R}(q_{old})) + L_D(\dot{q} + \mathcal{R}(\dot{q}_{old})), \end{aligned}$$

DOI: 10.1002/rnc

where appropriate positive definite matrices $L_P, L_D \in \mathbb{R}^{m\times m}$ denote the PD gains. Using this idea, the iteration law in Eq. (22) is reduced to

$$
\begin{cases}
q_{(3i+1)}(t^0) &= q_{(3i)}(t^1) \\
\dot{q}_{(3i+1)}(t^0) &= -\dot{q}_{(3i)}(t^1) \\
\bar{u}_{(3i+1)} &= L_P(q_{(3i+1)} - \mathcal{R}(q_{(3i)})) + L_D(\dot{q}_{(3i+1)} + \mathcal{R}(\dot{q}_{(3i)})) \\
\rho_{(3i+1)} &= \alpha(\hat{\rho}_{(3i)})
\end{cases}
\begin{cases}
q_{(3i+2)}(t^0) &= q_{(3i)}(t^1) \\
\dot{q}_{(3i+2)}(t^0) &= -\dot{q}_{(3i)}(t^1) \\
\bar{u}_{(3i+2)} &= L_P(q_{(3i+2)} - \mathcal{R}(q_{(3i)})) + L_D(\dot{q}_{(3i+2)} + \mathcal{R}(\dot{q}_{(3i)})) \\
\rho_{(3i+2)} &= \rho_{(3i)} + \epsilon_{(i)}\nabla_\eta \hat{\Gamma}(\hat{\rho}_{(3i)}, \eta_{(3i)})
\end{cases}
\begin{cases}
q_{(3i+3)}(t^0) &= q_{(0)}(t^0) \\
\dot{q}_{(3i+3)}(t^0) &= \dot{q}_{(0)}(t^0) \\
\bar{u}_{(3i+3)} &\equiv 0_{m\times 1} \\
\rho_{(3i+3)} &= \alpha\left(\hat{\rho}_{(3i)} - K_{\rho(i)}\left(\nabla_\rho \hat{\Gamma}(\hat{\rho}_{(3i)}, \eta_{(3i)}) + \frac{1}{\epsilon_{(i)}}(\eta_{(3i+2)} - \eta_{(3i+1)})\right)\right)
\end{cases}
\tag{39}
$$

Thus, a concrete iteration law of IFT for mechanical systems is obtained.

Remark 1

Basically, the proposed iteration law is to adjust the design parameters contained in the Hamiltonian function and elements of the dissipation matrix of the closed-loop system. For the parameters not directly dealt with the proposed method can be tuned via conventional IFT method, e.g., [15, 17]. Suppose that a tuning parameter $\rho \in \mathbb{R}^s$ is dealt with the proposed method, and another parameter $\kappa \in \mathbb{R}^r$ is not. Then, the number of experiments required for one step iteration of the gradient method in the conventional IFT method is $1 + r + s$, whereas that required for the proposed method is $3 + r$ since additional r experiments are needed to execute conventional IFT method in addition to the 3 step given in the iteration law (22) or (39). Therefore, the proposed method requires less number of experiments when $s > 2$. This analysis is summarized in Table I. Furthermore, since the ILC method in the authors' former result depends on the very same property, namely, the variational symmetry of Hamiltonian systems, the proposed method can be applied to simultaneous learning control with IFT and ILC [22, 24].

5. NUMERICAL EXAMPLE

This section demonstrates the effectiveness of the proposed method via numerical simulations. Here, we consider a two-link robot manipulator moving on a horizontal plane depicted in Fig. 4 and the PD feedback controller. The objective of this section is to tune the PD feedback gains by the proposed method so that possibly fast regulation of the initial response is achieved. We also compare the performance of the proposed method with those achieved by some conventional methods to clarify the advantages of the proposed method.

DOI: 10.1002/rnc

Table I. The required number of experiments in 1 step parameter estimation

	Existing method		Proposed method	
Number of parameter included in the Hamiltonian function and/or dissipation matrix (s)	1	s	1	2
Number of parameter exclude from the Hamiltonian function and/or dissipation matrix (r)		r		r
Required number of experiments	$1+s+r$		$3+r$	

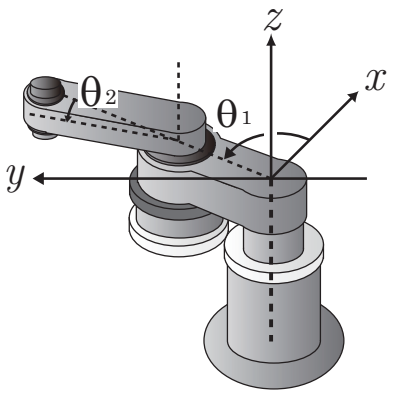

Figure 4. Two-link robot manipulator moving on a horizontal plane

Table II. Physical parameters

m_i	Mass of the ith link	[kg]
l_i	Length of the ith link	[m]
l_{ci}	Length to the center of gravity	[m]
$\bar{I}_i$	Inertia of the ith link	[kg m^2]
d_i	Friction coefficient of the ith link	[Nms/rad]

5.1. Description of the plant system

As in Fig. 4, the joint angles of the first and the second links of the manipulator are denoted by θ_1 and θ_2, respectively. The physical parameters of this apparatus are summarized in Table II. The dynamics of this apparatus is described by a typical mechanical system (23), where

DOI: 10.1002/rnc

$q = (q_1, q_2)^\top := (\theta_1, \theta_2)^\top \in \mathbb{R}^2$ and $p = (p_1, p_2)^\top := M(q)\dot{q} \in \mathbb{R}^2$ with the inertia matrix

$$
\begin{aligned}
M(q) &= \begin{pmatrix} m_{11}(q_2) & m_{12}(q_2) \\ m_{12}(q_2) & m_{22} \end{pmatrix}, \\
m_{11}(q_2) &:= \bar{I}_1 + \bar{I}_2 + m_1 l_{c1}^2 + m_2(l_1^2 + l_{c2}^2 + 2 l_1 l_{c2} \cos q_2), \\
m_{12}(q_2) &:= \bar{I}_2 + m_2(l_{c2}^2 + l_1 l_{c2} \cos q_2) \\
m_{22} &:= \bar{I}_2 + m_2 l_{c2}^2
\end{aligned}
$$

and the dissipation matrix $R_D = \mathrm{diag}\{d_1, d_2\}$, respectively, where $\mathrm{diag}\{\cdot\}$ denotes a (block) diagonal matrix. The state and the Hamiltonian are given by $x = (q^\top, p^\top)^\top \in \mathbb{R}^4$ and

$$
H(q, p, u) = \frac{1}{2} p^\top M(q)^{-1} p - u^\top q,
$$

where the potential energy is $U(q) = 0$ since the manipulator moves on a horizontal plane. Now, we consider the PD controller for the system. As mentioned in Section 4, the practical PD controller in (28) is equipped to simultaneously optimize both of the P feedback gain and D feedback gain.

For simplicity, suppose the feedback gain matrices to be $K_p = \mathrm{diag}\{K_{P1}, K_{P2}\}$ and $K_D = \mathrm{diag}\{K_{D1}, K_{D2}\}$, respectively, and define the tuning parameter as

$$
\rho = (\rho_1, \rho_2, \rho_3, \rho_4)^\top := (K_{P1}, K_{P2}, K_{D1}, K_{D2})^\top \in \mathbb{R}^4.
$$

Then, from Eqs. (33) and (34), the closed-loop system of the manipulator with the practical PD feedback controller is described by a Hamiltonian system with tuning parameter (14) as $\eta = \Sigma_{\mathfrak{h}}^{\chi_{t^0}, \bar{u}}(\rho)$:

$$
\dot{\chi} := \begin{pmatrix} \dot{q} \\ \dot{p} \\ \dot{\bar{\sigma}} \end{pmatrix} = \begin{pmatrix} 0_{2\times 2} & I_2 & 0_{2\times 2} \\ -I_2 & -R_D & 0_{2\times 2} \\ 0_{2\times 2} & 0_{2\times 2} & -I_2 \end{pmatrix} \begin{pmatrix} \frac{\partial \mathcal{H}(\chi, \bar{u}, \rho)}{\partial q}^\top \\ \frac{\partial \mathcal{H}(\chi, \bar{u}, \rho)}{\partial p}^\top \\ \frac{\partial \mathcal{H}(\chi, \bar{u}, \rho)}{\partial \bar{\sigma}}^\top \end{pmatrix}, \quad \chi_{t^0} = \begin{pmatrix} q(t^0) \\ p(t^0) \\ \bar{\sigma}(t^0) \end{pmatrix} = \begin{pmatrix} q_{t^0} \\ p_{t^0} \\ \bar{\sigma}_{t^0} \end{pmatrix},
$$

$$
\begin{aligned}
\mathcal{H}(\chi, \bar{u}, \rho) =& \frac{1}{2} p^\top M(q)^{-1} p + \frac{1}{2} q^\top \mathrm{diag}\{\rho_1, \rho_2\} q + \frac{1}{2\tau} \left(\mathrm{diag}\{\rho_3^{-\frac{1}{2}}, \rho_4^{-\frac{1}{2}}\} \bar{\sigma} + q \right)^\top \mathrm{diag}\{\rho_3, \rho_4\} \\
& \times \left(\mathrm{diag}\{\rho_3^{-\frac{1}{2}}, \rho_4^{-\frac{1}{2}}\} \bar{\sigma} + q \right) - \bar{u}^\top q,
\end{aligned}
$$

$$
\eta = \begin{pmatrix} \eta_1 \\ \eta_2 \\ \eta_3 \\ \eta_4 \end{pmatrix} = \begin{pmatrix} -\displaystyle\int_{t^0}^{t^1} \frac{q_1^2}{2} \, \mathrm{d}t \\ -\displaystyle\int_{t^0}^{t^1} \frac{q_2^2}{2} \, \mathrm{d}t \\ -\displaystyle\int_{t^0}^{t^1} \frac{q_1^2}{2\tau} + \frac{q_1 \bar{\sigma}_1}{2\tau\sqrt{K_{D1}}} \, \mathrm{d}t \\ -\displaystyle\int_{t^0}^{t^1} \frac{q_2^2}{2\tau} + \frac{q_2 \bar{\sigma}_2}{2\tau\sqrt{K_{D2}}} \, \mathrm{d}t \end{pmatrix}.
$$

DOI: 10.1002/rnc

In order to guarantee that the PD gains are optimized such that all of them remain non-negative, we equip the following differentiable constraint function:

$$F_1(v;\epsilon_v) := \begin{cases} 0 & (v<0) \\ -\dfrac{v^3}{\epsilon_v^2}+\dfrac{2v^2}{\epsilon_v} & (0\le v<\epsilon_v) \\ v & (v\le\epsilon_v) \end{cases} \tag{40}$$

with a sufficiently small positive constant ϵ_v. Then, the parameter constraints are characterized by

$$\rho=\alpha(\hat{\rho})=(F_1(\rho_1,\epsilon_v),F_1(\rho_2,\epsilon_v),F_1(\rho_3,\epsilon_v),F_1(\rho_4,\epsilon_v))^\top.$$

Remark 2
When a parameter ρ should be optimized with in the prescribed range $[\underline{\rho},\overline{\rho}]$, a possible constraint function

$$F_2(v;\underline{\rho},\overline{\rho}) := \frac{\overline{\rho}-\underline{\rho}}{2}\tanh\left(\frac{2v-\overline{\rho}-\underline{\rho}}{\overline{\rho}-\underline{\rho}}\right)+\frac{\overline{\rho}+\underline{\rho}}{2}$$

can be available.

Here, let us take a cost function as

$$\begin{aligned}\hat{\Gamma}(\hat{\rho},\eta) &= \sum_{i=1}^{2}\left(\lambda_{\eta_i}|\eta_i|+\frac{\lambda_{\rho_i}}{2}\hat{\rho}_i^2+\frac{\lambda_{\rho_{i+2}}}{2}\hat{\rho}_{i+2}^2\right) \\ &= \sum_{i=1}^{2}\left(\frac{\lambda_{\eta_i}}{2}\int_{t^0}^{t^1}|q_i|^2\,\mathrm{d}t+\frac{\lambda_{\rho_i}}{2}{K_{Pi}}^2+\frac{\lambda_{\rho_{i+2}}}{2}{K_{Di}}^2\right)\end{aligned} \tag{41}$$

so that fast regulation of the initial response is optimally achieved, where the positive constants λ_{η_i}'s $(i=1,2)$ and λ_{ρ_i}'s $(i=1,2,3,4)$ are weighting constants.

Remark 3
The cost function (41) only includes the regulation term with respect to the joint angles q. However, we have already proposed a supplementary method based on a pseudo adjoint of the time derivative operator in [22], which enables cost functions to include $\dot{q}$. Thus, the angular velocities can be simultaneously regulated as well.

5.2. *Application of the proposed method*

For the cost function (41), the iteration law follows from Eq. (39) with

$$\begin{aligned}\nabla_\eta\hat{\Gamma} &= (\lambda_{\eta_1}\,\mathrm{sgn}(\eta_1),\ \lambda_{\eta_2}\,\mathrm{sgn}(\eta_2),\ 0,\ 0)^\top, \\ \nabla_{\hat{\rho}}\hat{\Gamma} &= (\lambda_{\rho_1}\hat{\rho}_1,\ \lambda_{\rho_2}\hat{\rho}_2,\ \lambda_{\rho_3}\hat{\rho}_3,\ \lambda_{\rho_4}\hat{\rho}_4,\ )^\top,\end{aligned}$$

where $\mathrm{sgn}(\cdot)$ represents the signum function. We apply the proposed iteration procedure to the robot manipulator in Fig. 4. The concrete parameters used in the simulation are $m_1=m_2=1$ kg, $l_1=1, l_{c1}=0.5, l_2=2, l_{c2}=1$ m, $\bar{I}_1=8.3\times10^{-2}, \bar{I}_2=3.3\times10^{-1}$ kg m^2 and $d_1=d_2=0.5$ Nms/rad.

DOI: 10.1002/rnc

The time interval is set to $[t^0, t^1] = [0, 4]$ s. We utilize the following design parameters with respect to the weighting constants for the cost function (41) as $\lambda_{\eta_1} = \lambda_{\eta_2} = 10$, $\lambda_{\rho_1} = \lambda_{\rho_2} = 2.0 \times 10^{-4}$, $\lambda_{\rho_1} = \lambda_{\rho_2} = 2.0 \times 10^{-3}$. In this simulation, we proceed 250 steps of the learning procedure, which means total 750 experiments are executed. The initial condition of the manipulator is set to $(q_{1t^0}, q_{2t^0}, \dot{q}_{1t^0}, \dot{q}_{2t^0}) = (\pi/2, \pi/2, 0, 0)$, and that of the filtered derivative in (29) is set to $(\sigma_{t^0}, \dot{\sigma}_{t^0}) = (0, 0)$. The initial values of the tuning parameters are chosen as $\rho_{(0)} = (30, 30, 5, 5)$. The design parameters with respect to the iteration law (39) are set to $K_{\rho(\cdot)} = \mathrm{diag}(2.0 \times 10^2, 2.0 \times 10^2, 10, 10)$ and $\epsilon_{(\cdot)} = 2$, and that with respect to the saturation function F_1 in (40) as $\epsilon_v = 1.0 \times 10^{-3}$. The constant parameter τ in the low-pass filter in (28) is set to 0.01.

Under these circumstances, Figs. 5-8 show the results. Figure 5 depicts the history of the cost function (41) along the iteration. Since the cost function $\hat{\Gamma}$ decreases monotonically, it is concluded that the learning procedure works well, and at least a local minimum is achieved smoothly. Figure 6 exhibits the learning results of the tuning parameters. It shows that all the parameters converge to optimal values. The resultant cost is 8.478, and the resultant parameters are $K_{P1} = 48.553$, $K_{P2} = 36.518$, $K_{D1} = 13.854$ and $K_{D2} = 12.251$. Figure 7 depicts the histories of the costs with respect to q_i's, that is, $\lambda_{\eta_i}/2 \int_{t^0}^{t^1} |q_i|^2 \, \mathrm{d}t$, $(i = 1, 2)$. In Fig. 8, the initial and resultant responses of the joint angles are shown, respectively. From Figs. 7-8, it is concluded that fast regulation of the initial response of the manipulator is optimally achieved.

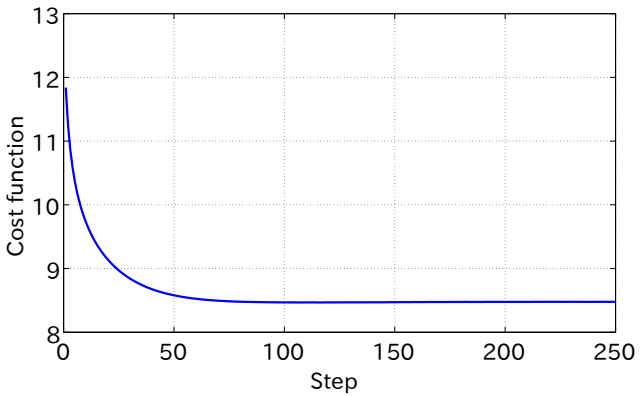

Figure 5. Cost function

5.3. *Comparison with conventional IFT methods*

In this subsection, we apply the conventional IFT methods to the same problem in order to compare the proposed method with them. Here, we consider IFT methods in [15, 17]. For this numerical example, we suppose the output to be $y = (q^\top, \dot{q}^\top)^\top$, and then the PD controller (25) is described by

$$u = C(\rho, y, r) = -\begin{pmatrix} K_{P1} & 0 & K_{D1} & 0 \\ 0 & K_{P2} & 0 & K_{D2} \end{pmatrix} y + r,$$

DOI: 10.1002/rnc

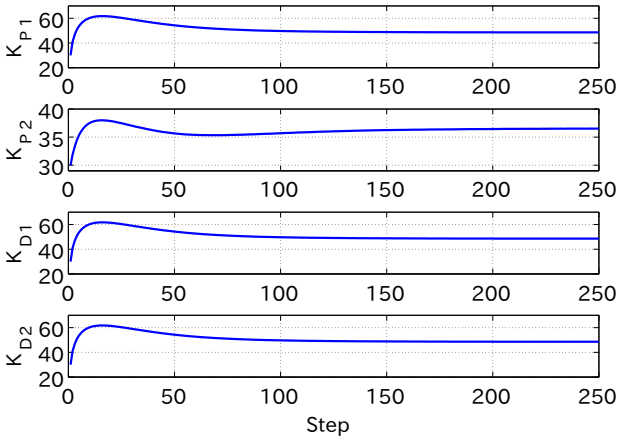

Figure 6. Learning results of $\hat{\rho}_i$, $(i = 1, \cdots, 4)$ $(\hat{\rho}_1 = K_{P1}, \hat{\rho}_2 = K_{P2}, \hat{\rho}_3 = K_{D1}$ and $\hat{\rho}_4 = K_{D2})$

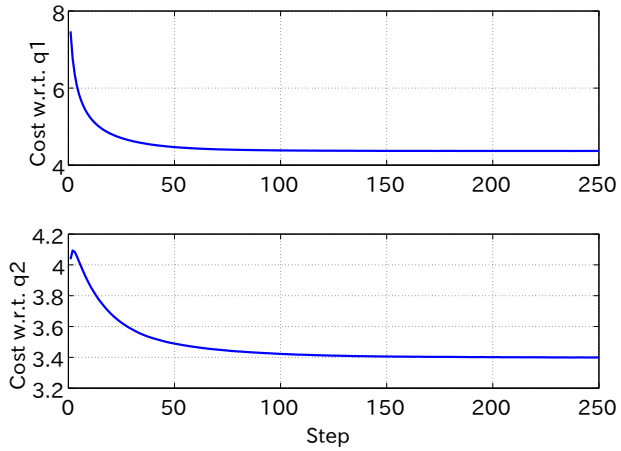

Figure 7. Cost with respect to q_i $(\lambda_{\eta_i}/2 \int_{t^0}^{t^1} |q_i|^2 \, \mathrm{d}t)$, $(i = 1, 2)$

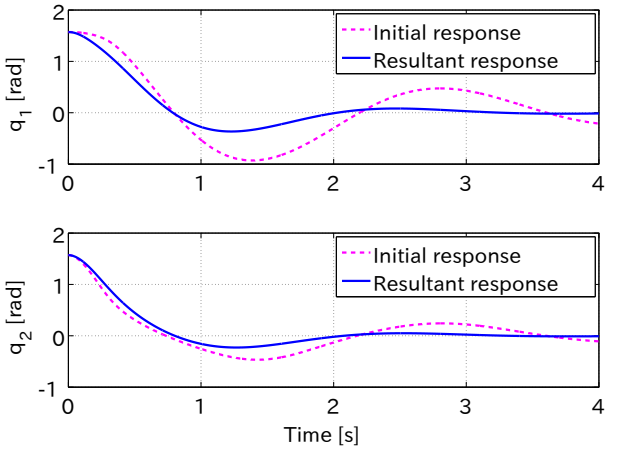

Figure 8. Learning results of q_1 and q_2

DOI: 10.1002/rnc

where $r \in L_2^2[t^0, t^1]$ denotes a reference signal. Subsequently, the resultant iteration laws in [15, 17] are reduced to the same one summarized as follows:

$$
\begin{cases} r_{1(5i+1)} &= -\epsilon_{(i)} q_{1(5i)} \\ r_{2(5i+1)} &\equiv 0 \\ \rho_{(5i+1)} &= \rho_{(5i)} \end{cases}
\begin{cases} r_{1(5i+2)} &\equiv 0 \\ r_{2(5i+2)} &= -\epsilon_{(i)} q_{2(5i)} \\ \rho_{(5i+2)} &= \rho_{(5i)} \end{cases}
\begin{cases} r_{1(5i+3)} &= -\epsilon_{(i)} \dot{q}_{1(5i)} \\ r_{2(5i+3)} &\equiv 0 \\ \rho_{(5i+3)} &= \rho_{(5i)} \end{cases}
\begin{cases} r_{1(5i+4)} &\equiv 0 \\ r_{2(5i+4)} &= -\epsilon_{(i)} \dot{q}_{2(5i)} \\ \rho_{(5i+4)} &= \rho_{(5i)} \end{cases}
$$

$$
\begin{cases} r_{(5i+5)} &\equiv 0_{2\times 1} \\ \rho_{j(5i+5)} &= \rho_{j(5i)} - K_{\rho_j(i)} \left(\lambda_{\rho_j} \rho_{j(5i)} + \int_{t^0}^{t^1} q_{(5i)}^{\top} \Lambda_{\eta} \frac{(q_{(5i+j)} - q_{(5i)})}{\epsilon_{(i)}} \, \mathrm{d}t \right), \quad (j = 1, \ldots, 4) \end{cases} . \tag{42}
$$

For the linear systems, the author in [15] proposes an efficient algorithm reducing the number of experiments required for the gradient calculation by using commutativity of linear operators. However, for a nonlinear system as this example considers, the required number of the gradient experiments per one step iteration is equal to the number of elements in ρ. Besides, the authors in [17] propose a similar IFT algorithm for nonlinear systems, and this method also has the same issue on the required number of the gradient experiments. Although the literature [17] proposes another IFT method, which requires only two gradient experiments per one step iteration, it requires identification of a model of the linearization of the closed-loop system around its operating trajectory, instead.

We consider the same cost function and initial conditions as in Subsection 5.2 with the same parameters. We proceed 250 steps of the learning procedure with the iteration law (42). Although the number of learning steps is the same as in Subsection 5.2, the total number of necessary experiments is 1250 in this case. The design parameters with respect to the iteration law (42) are set to $K_{\rho(\cdot)} = \mathrm{diag}(1.0 \times 10^2, 1.0 \times 10^2, 5, 5)$ and $\epsilon_{(\cdot)} = 1$. They are chosen so that similar convergence speed and optimization performance, namely, the resultant cost can be achieved for a fair comparison. Figure 9 depicts the history of the cost function (41) along the iteration. Figure 11 exhibits the learning results of the tuning parameters. The resultant cost is 8.538, and the resultant parameters are $K_{P1} = 49.721$, $K_{P2} = 35.330$, $K_{D1} = 12.990$ and $K_{D2} = 8.378$. Figure 10 depicts the histories of the costs with respect to q_i's, that is, $\lambda_{\eta_i}/2 \int_{t^0}^{t^1} |q_i|^2 \, \mathrm{d}t$, $(i = 1, 2)$. Figure 12 shows the initial and resultant responses of the joint angles, respectively. From Figs. 10-12, it is concluded that the iteration law (42) also works well, but the total number of experiments is much larger than that of the proposed method. We summarize the comparison results in Table III.

DOI: 10.1002/rnc

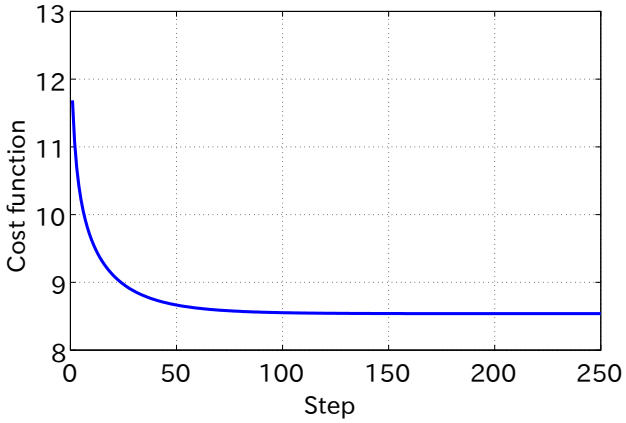

Figure 9. Cost function

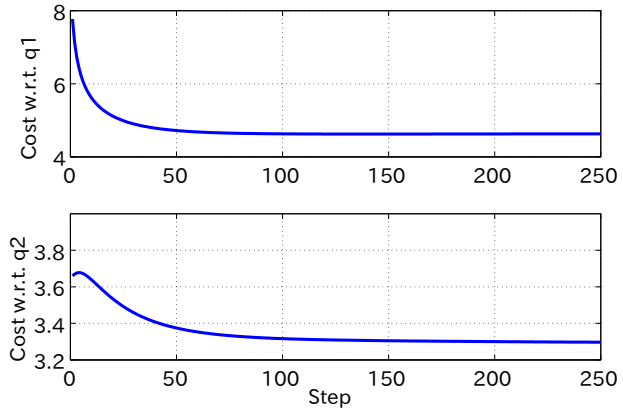

Figure 10. Cost with respect to q_i $(\lambda_{\eta_i}/2 \int_{t^0}^{t^1} |q_i|^2 \, \mathrm{d}t)$, $(i = 1, 2)$

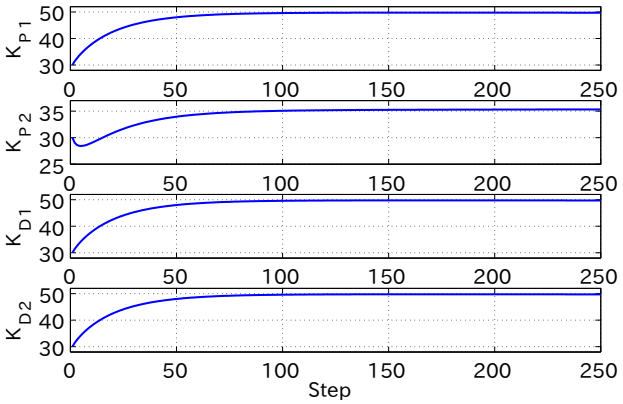

Figure 11. Learning results of $\hat{\rho}_i$, $(i = 1, \cdots, 4)$ $(\hat{\rho}_1 = K_{P1}, \hat{\rho}_2 = K_{P2}, \hat{\rho}_3 = K_{D1}$ and $\hat{\rho}_4 = K_{D2})$

DOI: 10.1002/rnc

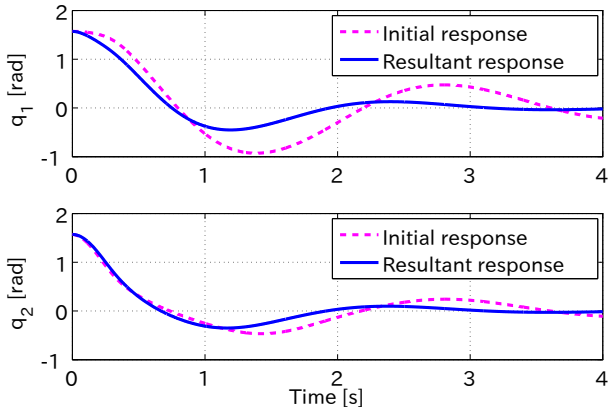

Figure 12. Learning results of q_1 and q_2

Table III. Summary of the comparison results

	Existing methods [15, 17]	Proposed method
Total learning steps	250	250
Required experiments	1250	**750**
Achieved cost	8.538	**8.478**
Resultant gains	$K_{P1} = 49.721$ $K_{P2} = 35.330$ $K_{D1} = 12.990$ $K_{D2} = 8.378$	$K_{P1} = 48.553$ $K_{P1} = 36.518$ $K_{D1} = 13.854$ $K_{D2} = 12.251$

6. CONCLUSION

This paper has proposed a new IFT method for Hamiltonian systems. We have derived a modified variational symmetry of Hamiltonian systems, which can be used for estimating the gradient of a given cost function with respect to the finite number of parameters. Then, a novel IFT algorithm has been developed based on this property. We have also provided a method to optimize the elements of the dissipation matrix, which does not directly appear in the Hamiltonian function, by equipping a dynamic feedback of the generalized coordinate. Moreover, we have provided an IFT algorithm considering parameter constraints so that tuning parameters can be optimized within a prescribed search range by adapting the idea of ILC method with input saturation technique. Finally, a numerical simulation of a two-link robot manipulator including comparison with the conventional IFT methods, has exhibited the effectiveness of the proposed method.

The advantageous features of this method are as follows. First, it requires less number of gradient experiments compared with the conventional IFT methods for nonlinear systems. Second, it can optimize not only feedback gains, but also other adjustable parameters of the plant system itself appearing in the Hamiltonian function, such as the mass, inertia, link length, stiffness and so on. Third, it can be applied to simultaneous learning control with IFT and ILC based on the variational symmetry.

DOI: 10.1002/rnc

ACKNOWLEDGEMENT

This work was supported by JSPS KAKENHI Grant Numbers JP17H03282 and JP18K04202.

REFERENCES

[1] van der Schaft AJ. *L_2-gain and Passivity Techniques in Nonlinear Control*, vol. 218. Lecture Notes on Control and Information Science: Berlin, 1996.

[2] Ortega R, van der Schaft AJ, Maschke B, Escobar G. Interconnection and damping assignment passivity-based control of port-controlled Hamiltonian systems. *Automatica* 2002; **38**(4):585–596.

[3] Fujimoto K, Sakurama K, Sugie T. Trajectory tracking control of port-controlled Hamiltonian systems via generalized canonical transformations. *Automatica* 2003; **39**(12):2059–2069.

[4] Satoh S, Fujimoto K. Passivity based control of stochastic port-Hamiltonian systems. *IEEE Trans. Autom. Contr.* 2013; **58**(5):1139–1153.

[5] Nageshrao SP, Lopes GAD, Jeltsema D, Babuška R. Port-Hamiltonian systems in adaptive and learning control: A survey. *IEEE Trans. Autom. Contr.* 2016; **61**(5):1223–1238.

[6] Satoh S. Input-to-state stability of stochastic port-Hamiltonian systems using stochastic generalized canonical transformations 2017. To appear in *Int. J. Robust and Nonlinear Control*.

[7] Arimoto S, Kawamura S, Miyazaki F. Bettering operation of robotics. *J. Robotic Systems* 1984; **1**(2):123–140.

[8] Moore KL. *Iterative Learning Control for Deterministic Systems*. Advances in Industrial Control, Springer-Verlag: London, 1993.

[9] Chen Y, Wen C. *Iterative Learning Control: Convergence, Robustness and Applications*, *Lecture Notes on Control and Information Science*, vol. 248. Springer-Verlag, 1999.

[10] Bristow DA, Tharayil M, Alleyne AG. A survey of iterative learning control. *IEEE Control Systems Magazine* 2006; **26**(3):96–114.

[11] Hjalmarsson H, Gunnarsson S, Gevers M. A convergent iterative restricted complexity control design scheme. *Proc. 33rd IEEE Conf. on Decision and Control*, 1994; 1735–1740.

[12] Bruyne FD. Iterative feedback tuning for MIMO systems. *Proc. 2th Int. Symposium on Intelligent Automation and Control*, 1997; 179.1–179.8.

[13] Hjalmarsson H, Gevers M, Gunnarsson S, Lequin O. Iterative feedback tuning: theory and applications. *IEEE Control Systems* 1998; **18**(4):26–42.

[14] Hamamoto K, Sugie T. Construction of suboptimal controllers via iterative feedback tuning. *Proc. European Control Conference*, 1999; 1766–1771.

[15] Hjalmarsson H. Iterative feedback tuning - an overview. *Int. J. Adaptive Control and Signal Processing* 2002; **16**:373–395.

[16] Sjöberg J, Agarwal M. Model-free repetitive control design for nonlinear systems. *Proc. 35th IEEE Conf. on Decision and Control*, 1996; 2824–2829.

[17] Bruyne FD, Anderson BDO, Gevers M, Linard N. Iterative controller optimization for nonlinear systems. *Proc. 36th IEEE Conf. on Decision and Control*, vol. 4, 1997; 3749–3754.

DOI: 10.1002/rnc

[18] Benosman M. Multi-parametric extremum seeking-based iterative feedback gains tuning for nonlinear control. *Int. J. Robust and Nonlinear Control* 2016; **26**(18):4035–4055.

[19] Sprangers O, Babuška R, Nageshrao SP, Lopes GAD. Reinforcement learning for port-hamiltonian systems. *IEEE Trans. Cybernetics* 2015; **45**(5):1017–1027.

[20] Fujimoto K, Sugie T. Iterative learning control of Hamiltonian systems: I/O based optimal control approach. *IEEE Trans. Autom. Contr.* 2003; **48**(10):1756–1761.

[21] Fujimoto K, Horiuchi T, Sugie T. Optimal control of Hamiltonian systems with input constraints via iterative learning. *Proc. 42nd IEEE Conf. on Decision and Control*, 2003; 4387–4392.

[22] Satoh S, Fujimoto K, Hyon S. Gait generation via unified learning optimal control of Hamiltonian systems. *Robotica* 2013; **31**(5):717–732.

[23] Fujimoto K, Koyama I. Iterative feedback tuning for Hamiltonian systems. *Proc. 17th IFAC World Congress*, 2008; 15 678–15 683.

[24] Satoh S, Fujimoto K, Saeki M. Transition to an optimal periodic gait by simultaneous input and parameter optimization method of Hamiltonian systems. *Artificial Life and Robotics* 2016; **21**(3):258–267.

[25] Pontryagin LS, Boltyanskii VG, Gamkrelidze RV, Mishchenko EF. *The Mathematical Theory of Optimal Processes*. John Wiley and Sons: New York, 1962.

[26] Crouch PE, van der Schaft AJ. *Variational and Hamiltonian Control Systems*, *Lecture Notes on Control and Information Science*, vol. 101. Springer-Verlag: Berlin, 1987.

[27] Fujimoto K, Sugie T. Canonical transformation and stabilization of generalized Hamiltonian systems. *Systems & Control Letters* 2001; **42**(3):217–227.

[28] Åström KJ, Hägglund T. *PID Controllers: Theory, Design, and Tuning*. 2nd edn., ISA, 1995.

[29] Crowe J, et al. *PID Control New Identification and Design Methods*. Springer-Verlag: London, 2005.

[30] Ortega R, Spong M, Gómez-Estern F, Blankenstein G. Stabilization of a class of underactuated mechanical systems via interconnection and damping assignment. *IEEE Trans. Autom. Contr.* 2002; **47**(8):1218–1233.

DOI: 10.1002/rnc